CrossMark

Associations of hemodynamics, morphology, and patient characteristics with aneurysm rupture stratified by aneurysm location

Felicitas J. Detmer[1] (ID) · Bong Jae Chung[1] · Carlos Jimenez[2] · Farid Hamzei-Sichani[3] · David Kallmes[4] ·
Christopher Putman[5] · Juan R. Cebral[1]

Abstract

Purpose The mechanisms of cerebral aneurysm rupture are not fully understood. We analyzed the associations of hemodynamics, morphology, and patient age and gender with aneurysm rupture stratifying by location.

Methods Using image-based models, 20 hemodynamic and 17 morphological parameters were compared in 1931 ruptured and unruptured aneurysms with univariate logistic regression. Rupture rates were compared between males and females as well as younger and older patients and bifurcation versus sidewall aneurysms for different aneurysm locations. Subsequently, associations between hemodynamics and morphology and patient as well as aneurysm characteristics were analyzed for aneurysms at five locations.

Results Compared to unruptured aneurysms, ruptured aneurysms were characterized by a more irregular shape and were exposed to a more adverse hemodynamic environment described by faster flow, higher wall shear stress, more oscillatory shear, and more unstable and complex flows. These associations with rupture status were consistent for different aneurysm locations. Rupture rates were significantly higher in males at the internal carotid artery (ICA) bifurcation, ophthalmic ICA, and the middle cerebral artery (MCA) bifurcation. At the anterior communicating artery (ACOM) and MCA bifurcation, they were significantly higher for younger patients. Bifurcation aneurysms had significantly larger rupture rates at the MCA and posterior communicating artery (PCOM). In these groups with higher rupture rates, aneurysms were characterized by adverse hemodynamics and more complex shapes.

Conclusion Hemodynamic and morphological differences between ruptured and unruptured aneurysms are consistent across locations. Adverse morphology and hemodynamics are related to rupture as well as younger age, male gender, and bifurcation aneurysms.

Keywords Aneurysm · Risk factors · Hemodynamics · Morphology · CFD

Abbreviations

CFD	Computational fluid dynamics	ROC	Receiver operating characteristic
ICA	Internal carotid artery	ACOM	Anterior communicating artery
VA	Vertebral artery	ICA-OPH	Ophthalmic segment of the ICA
		ICA-BIF	Internal carotid artery bifurcation

✉ Felicitas J. Detmer
   fdetmer@gmu.edu

[1] Bioengineering Department, Volgenau School of Engineering, George Mason University, 4400 University Drive, Fairfax, VA 22030, USA

[2] Neurosurgery Department, University of Antioquia, Medellin, Colombia

[3] Department of Neurological Surgery, University of Massachusetts, Worcester, MA, USA

[4] Department of Radiology, Mayo Clinic, Rochester, MN, USA

[5] Interventional Neuroradiology Unit, Inova Fairfax Hospital, Falls Church, VA, USA

⚡ Springer

PCOM	'Posterior communicating artery
MCA	Middle cerebral artery
MCA-DIST-PROX	Without the MCA-bifurcation
WSS	Wall shear stress
OSI	Oscillatory shear index

Introduction

Cerebral aneurysms are a common vascular disease occurring in about 2–3% of the population [1]. While remaining asymptomatic in most cases, the rupture of an aneurysm leads to hemorrhagic stroke which is associated with high mortality and morbidity [2, 3]. Nowadays, an increasing number of unruptured aneurysms is diagnosed as incidental findings [4]. Treatment decisions of incidentally diagnosed aneurysms require the assessment of a patient's individual aneurysm rupture risk. The mechanisms that lead to aneurysm rupture are however not yet fully understood making treatment decisions difficult. In recent years, computational fluid dynamics (CFD) simulations have become more and more popular for the assessment of hemodynamic factors associated with aneurysm development, growth, and rupture [5]. Typically, these studies are based on patient data from a single center and comprise relatively small patient cohorts of often less than 200 patients [6–9]. In the presented study, we used data of aneurysms obtained from six hospitals of approximately 1900 cases. Besides hemodynamic risk factors, it is known that the aneurysm rupture risk differs by aneurysm location with a higher rupture risk for aneurysms of the posterior circulation [10]. Furthermore, aneurysm hemodynamics are influenced by the aneurysm geometry. In this context, several morphological risk factors have previously been suggested [6, 8, 9]. The aim of this study was the identification of hemodynamic and morphological risk factors for aneurysm rupture as well as the assessment of the association of gender and age with aneurysm rupture rates using a large patient cohort. Based on our previous study [11], we hypothesized that higher rupture rates for one or the other population would be associated with more adverse aneurysm hemodynamics characterized by more complex flows with concentrated wall shear stress (WSS) and more complex aneurysm shapes. The analysis was stratified by aneurysm location to avoid this potential confounding factor.

Materials and methods

Patient and image data

After exclusion of fusiform aneurysms, data of 1265 patients having 1931 saccular intracranial aneurysms with known rupture status were available. They include 3-dimensional rotational angiography (3DRA) images of the aneurysm and the surrounding vasculature, as well as information about the patient (age and gender) and the aneurysm location in the cerebral vasculature. All the data has been anonymized.

Hemodynamic modeling

Patient-specific CFD models were performed as previously described [12]. In short, CFD models were constructed from the angiographic images of the aneurysm and the surrounding vasculature. In the models, arteries were cut perpendicularly to their axes for subsequent inlet and outlet definition. The vessels were modeled by unstructured grids with a maximum element size of 0.2 mm.

For the CFD simulations, pulsatile flow conditions derived from phase-contrast MR measurements in healthy subjects were scaled with a power law to the inlet vessel area. Depending on the location of the aneurysm, inflow boundary conditions were applied at the internal carotid artery (ICA) (for aneurysms in the anterior circulation) or the vertebral artery (VA) (for aneurysms in the posterior circulation) using the Womersly solution. Outflow boundary conditions consistent with Murray's law were applied. Blood was modeled as a Newtonian fluid with a density of 1.0 g/cm^3 and a viscosity of 0.04 P. Vessel walls were approximated as rigid. An in-house finite element solver was used to numerically solve the 3D incompressible Navier-Stokes equations. Two cardiac cycles with a heart rate of 60 beats per minute were calculated with 100 time steps per cardiac cycle and results from the second cycle were used for the hemodynamic characterizations.

Post processing

In the post processing step, 20 hemodynamic and 17 morphological variables, which have been described previously [12–15], were calculated from the computed flow field and the 3D geometrical model, respectively. They are presented in Tab. 1 in the Online Suppl. Material.

Statistical analysis

To assess the influence of hemodynamic conditions and aneurysm morphology on the aneurysm rupture risk, univariate logistic regression was performed for each of the 37 variables for subgroups of aneurysms stratified by aneurysm location. Furthermore, multivariate models, each including a hemodynamic or morphological variable, the categorical variable "aneurysm location" and a multiplicative interaction term of the two variables were fitted to analyze whether the influence of certain hemodynamic or morphological conditions on the aneurysm rupture risk could vary by aneurysm location. The statistical significance of the interaction term was assessed by an ANOVA analysis applied to the fitted model.

To identify whether the associations of the patient characteristics gender and age with aneurysm rupture could differ for aneurysms at different arteries, a test for an interaction term of "age" or "gender" with the variable "aneurysm location" was applied in the same way as described above for the hemodynamic and morphological parameters.

In order to compare rupture rates at different locations for aneurysms harbored by young versus old patients, patients were classified as "young" or "old" by fitting a univariate model for the variable "age" using the whole sample (all aneurysm locations) and selecting the optimal classification threshold as the age corresponding to the point on the receiver operating characteristic (ROC) curve with the smallest Euclidean distance to (0.1).

Subsequently, for each of 13 specified aneurysm locations, rupture rates were compared between aneurysms harbored by young versus old patients and female versus male patients. For the comparison, a Chi-square test was applied if the expected frequencies for all categories were greater than five; otherwise, Fisher's exact test was used. Based on the results of the Chi-square/Fisher's exact test, aneurysm locations were selected for further analysis of hemodynamic and morphological parameters with respect to gender, age, and rupture status by univariate logistic regression.

Similarly, differences in hemodynamics and morphology between sidewall and bifurcation aneurysms were compared at locations with significant differences in rupture rates for ruptured versus unruptured aneurysms based on Chi-square or Fisher/s exact test. For this analysis, only locations where both lateral and bifurcation aneurysms occur, were considered. These were the ophthalmic segment of the ICA (ICA-OPH), the anterior choroidal segment of the ICA (ICA-ACHOR), the middle cerebral artery (MCA), and the anterior cerebral artery and anterior communicating artery (ACA-ACOM), and the posterior communicating artery (PCOM). For PCOM aneurysms, aneurysms were classified as lateral versus bifurcation based on their angioarchitecture [16]. For all statistical analyses, a p value of 0.05 was considered as significant. In order to account for multiple testing, p values were also adjusted using the Benjamini-Hochberg procedure to limit the false discovery rate (FDR) [17]. For the analyses with respect to patient characteristics, the sample size was reduced from 1931 to 1640 due to missing patient information for a subset of cases. All statistical analysis was performed with scripts written in the R language [18].

Results

Overall, 558 out of the 1931 aneurysms were ruptured (rupture rate 0.29). The two locations with the highest rupture rates were the anterior communicating artery (ACOM, 169 out of 278, rupture rate 0.61) and the posterior communicating artery (144 out of 312, rupture rate 0.46). The lowest rupture rates were found for aneurysms located at the ophthalmic segment of the ICA (22 out of 280, rupture rate 0.07) and the MCA without the MCA-bifurcation (MCA-DIST-PROX, 5 out of 72, rupture rate 0.07, see Table 1).

Hemodynamics and morphology

Table 1 summarizes the results for the comparison of hemodynamic and morphological parameters by aneurysm location. When combining aneurysms of all locations, almost all of the 49 variables were associated with the aneurysm rupture status. Compared to unruptured aneurysms, ruptured aneurysms had a significantly larger inflow concentration index (ICI, $p < 0.001$), inflow rate into the aneurysm (Q, $p = 0.003$), kinetic energy (KE, $p < 0.001$), mean velocity (VE, $p = 0.001$), maximum wall shear stress (WSSmax, $p < 0.001$), mean WSS (WSSmean, $p = 0.009$), shear concentration index (SCI, $p < 0.001$), maximum oscillatory shear index (OSImax, $p < 0.001$), mean OSI (OSImean, $p < 0.001$), WSS in the aneurysm parent vessel (WSSves, $p < 0.001$), maximum normalized WSS (MWSSnorm, $p < 0.001$), vortex coreline length (corelen, $p < 0.001$), temporal flow stability (podent, $p < 0.001$), and peak velocity (Vmax, $p < 0.001$)). Besides, they were larger (Asize, $p < 0.001$) and had a larger aspect ratio (AR, $p < 0.001$), height (Aheight, $p < 0.001$), height-to-width ratio (HWR, $p < 0.001$), bottle-neck-factor (BF, $p < 0.001$), bulge location (BL, $p < 0.001$), size ratio (SizeR, $p < 0.001$), volume-to-ostium ratio (VOR, $p = 0.04$), convexity ratio (CR, $p < 0.001$), isoperimetric ratio (IPR, $p < 0.001$), non-sphericity index (NSI, $p < 0.001$), and L2 norm of mean surface curvatures (MLN, $p < 0.001$). In contrast, ruptured aneurysms had a significantly lower minimum WSS (WSSmin, $p < 0.001$), and mean WSS normalized by the WSS in the parent artery (WSSnorm, $p < 0.001$). With respect to the shape parameters, ruptured aneurysms had a smaller neck area (Narea, $p = 0.02$), diameter of the parent vessel (Vdiam, $p < 0.001$), and ellipticity index (EI, $p = 0.02$). When adjusting the p value for rejection of the null-hypothesis for multiple testing, the same variables remained significant (see Table 1). The p values and mean values in our data for the analyzed variables can be found in Tab. 2 in the Online Suppl. Material.

For the comparisons of hemodynamic and morphological variables by location, fewer parameters were significantly associated with the rupture status. However, all significant variables were consistently higher or lower for ruptured aneurysms throughout all locations. With respect to the interaction tests, significant interactions between the hemodynamic or morphological variable and aneurysm location were found for Vmax ($p = 0.02$), BL ($p = 0.008$), and MLN ($p = 0.03$, see also Tab. 3 in the Online Suppl. Material). The interaction

Table 1 Summary of univariate comparison of morphological and hemodynamic parameters by locations

	ACA	ACOM	BA-DIST-PROX	BA-TIP	ICA-ACHOR	ICA-BIF	ICA-CAV	ICA-OPH	ICA-SHYP	MCA-BIF	MCA-DIST-PROX	PCOM	VA	ALL
ICI														R*
Q							R							R*
KE							R							R*
SR														
VE							R							R*
VO														
VD														
WSSmax		R				R	R		R	R*		R*		R*
WSSmin		U*										U*		U*
WSSmean														R*
LSA												R		
SCI		R		R	R					R*				R*
OSImax	R	R							R	R*		R*		R*
OSImean										R*		R		R*
WSSves									R	R*		R*		R*
WSSnorm										U		U*		U*
MWSSnorm		R*			R									R*
corelen		R		R						R		R*		R*
podent	R													R*
Vmax		R				R	R		R	R*		R*		R*
Avol														
Asize	R									R		R*		R*
Nsize														
Narea														U*
AR	R	R*		R*		R				R*		R*		R*
Aheight	R											R*		R*
Awidth														
HWR		R*		R			R	R		R*		R*		R*
BF		R				R						R*		R*
BL	R		R		R							R*		R*
Vdiam		U						U						U*
SizeR	R	R*							R	R*		R*		R*
VOR														R*
CR												R		R*
EI														U*
NSI	R	R*		R					R	R*		R*		R*
MLN	R	R*		R*	R				R	R*		R*		R*
Sample Size	65	278	56	80	49	72	167	302	151	282	72	312	45	1931
Rupture Rate	34%	61%	20%	38%	14%	17%	4%	7%	17%	30%	7%	46%	40%	29%

ACA anterior cerebral artery, *ACOM* anterior communicating artery, *BA-DIST-PROX* basilar artery other than tip, *BA-TIP* tip of basilar artery, *ICA-ACHOR* internal carotid artery—anterior choroidal, *ICA-BIF* internal carotid artery bifurcation, *ICA-CAV* cavernous internal carotid artery, *ICA-OPH* internal carotid artery—ophthalmic, *ICA-SHYP* superior hypophyseal segment internal carotid artery, *MCA-BIF* middle cerebral artery bifurcation, *MCA-DIST-PROX* middle cerebral artery other than bifurcation, *PCOM* posterior communicating artery, *VA* vertebral artery. R and U indicate significantly positive and negative association of the variable with aneurysm rupture, respectively. Asterisks refer to significant difference after adjustment for multiple testing. Empty cells indicate no statistically significant difference. ALL refers to the results when combining aneurysms from all locations for the analysis

of the variables gender and aneurysm location was significant at 94% ($p = 0.06$), for age the p value was 0.01.

Gender and age

Based on the ROC of the univariate model for age, the optimal threshold was 55 years. Subsequently, patients having an age greater than 55 were classified as "old." Patients with an age of 55 or less were grouped as "young." Rupture rates were significantly higher for aneurysms harbored by young compared to old patients (37% vs. 25%, $p < 0.001$). When stratifying the comparison by locations, aneurysms of younger patients had significantly higher rupture rates at the ACOM (74% vs. 57%, $p = 0.01$), trunk of the basilar artery (BA-DIST-PROX, 40% vs. 10%, $p = 0.04$), bifurcation of the internal carotid artery (ICA-BIF, 31% vs 0%, $p = 0.002$), superior hypophyseal segment of the internal carotid artery (ICA-SHYP, 25% vs. 8%, $p = 0.01$), and the bifurcation of the MCA (MCA-BIF, 45% vs. 22%, $p < 0.001$, see Table 2). Only for the groups of aneurysms at the ACOM and MCA-BIF, the minimum number of cases per category (ruptured old, ruptured young, unruptured old, unruptured young) exceeded six. Therefore, aneurysms at the ACOM and MCA-BIF were selected for further comparison with respect to age groups. For ACOM aneurysms, 84

Table 2 Results of comparison of rupture rates in age groups by location

	Rupture rate young	Rupture rate old	p value	Method	Signf.	Sample size (young/old)
ACA	0.4	0.31	0.68	ChiSq		57 (25/32)
ACOM	0.74	0.57	0.01	ChiSq	*	228 (114/114)
BA-DIST-PROX	0.4	0.1	0.04	Fis	*	45 (15/30)
BA-TIP	0.5	0.38	0.50	ChiSq		61 (24/37)
ICA-ACHOR	0.23	0.07	0.23	Fis		41 (26/15)
ICA-BIF	0.31	0	0.002	Fis	*	58 (35/23)
ICA-CAV	0.02	0.04	1	Fis		129 (44/85)
ICA-OPH	0.08	0.07	0.96	ChiSq		275 (149/126)
ICA-SHYP	0.25	0.08	0.01	ChiSq	*	133 (59/74)
MCA-BIF	0.45	0.22	< 0.001	ChiSq	*	251 (102/149)
MCA-DIST-PROX	0.13	0.05	0.36	Fis		61 (23/38)
PCOM	0.52	0.45	0.29	ChiSq		265 (109/156)
VA	0.62	0.3	0.11	ChiSq		36 (16/20)

ChiSq refers to a comparison of rupture rates by a Chi-squares test, Fis to a comparison using Fisher's exact test

aneurysms belonging to the subgroup of young patients were ruptured, 30 were unruptured. Of the 114 aneurysms harbored by older patients, 65 were ruptured and 49 unruptured. For aneurysms located at the MCA-BIF, 33 and 116 aneurysms of the older patients were respectively ruptured and unruptured. In the subgroup of younger patients, 46 aneurysms were ruptured and 56 aneurysms were unruptured.

Aneurysms harbored by male patients had a significantly larger rupture rate compared to aneurysms of female patients independent of location (41% vs. 26%, $p < 0.001$) as well as at the ICA-BIF (45% vs. 13%, $p = 0.03$), the ICA-OPH (20% vs. 5%, $p = 0.002$), and the MCA-BIF (45% vs. 27%, $p = 0.02$, see Table 3). Since for the ICA-BIF and ICA-OPH, the maximum subgroup size for each category was 5 and 9, respectively, only aneurysms at the MCA-BIF were analyzed with

respect to differences in hemodynamic and morphological parameters by gender and rupture status. For aneurysms at this location, 26 (32) male aneurysms were ruptured (unruptured) and 53 female aneurysms were ruptured, 140 unruptured.

Gender and age by aneurysm location

When comparing hemodynamic and morphological parameters for aneurysms located at the ACOM and MCA-BIF separately, ruptured aneurysms had a larger maximum WSS ($p = 0.03$ and 0.04 for ACOM and MCA-BIF aneurysms, respectively), SCI ($p = 0.04$ and 0.01), maximum OSI ($p = 0.04$ and 0.002), vortex coreline length ($p = 0.02$ and 0.03) and, Vmax ($p = 0.03$ and 0.01) (Table 4). Furthermore, they had a larger AR ($p < 0.001$ and 0.003), SizeR ($p = 0.003$ and 0.007), NSI

Table 3 Results of comparison of rupture rates for subgroups of female and male aneurysms by location

	Rupture rate female	Rupture rate male	p value	Method	Signf.	Sample size (female/male)
ACA	0.31	0.44	0.48	ChiSq		57 (39/18)
ACOM	0.64	0.67	0.78	ChiSq		228 (143/85)
BA-DIST-PROX	0.17	0.33	0.35	Fis		45 (36/9)
BA-TIP	0.43	0.42	1	ChiSq		61 (49/12)
ICA-ACHOR	0.19	0	0.57	Fis		41 (36/5)
ICA-BIF	0.13	0.45	0.03	Fis	*	58 (47/11)
ICA-CAV	0.02	0.09	0.13	Fis		129 (107/22)
ICA-OPH	0.05	0.2	0.002	Fis	*	275 (231/44)
ICA-SHYP	0.17	0.09	0.53	Fis		133 (110/23)
MCA-BIF	0.27	0.45	0.02	ChiSq	*	251 (193/58)
MCA-DIST-PROX	0.06	0.18	0.22	Fis		61 (50/11)
PCOM	0.48	0.5	0.89	ChiSq		265 (221/44)
VA	0.44	0.45	1	Fis		36 (25/11)

ChiSq refers to a comparison of rupture rates by a Chi-squares test, Fis to a comparison using Fisher's exact test

Table 4 Summary of univariate comparison of morphological and hemodynamic parameters by subgroup for ACOM and MCA-BIF aneurysms

Comparison	ACOM				MCA-BIF						
	All_R_U	All_Y_O	Young_R_U	Old_R_U	All_R_U	All_Y_O	Young_R_U	Old_R_U	All_M_F	Fem_R_U	Male_R_U
ICI											
Q									M*		
KE								O_R	M*		
SR											
VE								O_R	M*		
VO									M		
VD											
WSSmax	R			O_R	R*			O_R	M		M_R
WSSmin	U*	O	Y_U								
WSSmean									M		
LSA											
SCI	R				R*						
OSImax	R		Y_R		R*		Y_R				M_R
OSImean					R*	Y	Y_R	O_R		F_R	M_R
WSSves				O_R	R*						M_R
WSSnorm					U		Y_U			F_U	
MWSSnorm	R*			O_R							M_R
corelen	R		Y_R		R				M		
podent											
Vmax	R				R*			O_R	M*		M_R
Avol											
Asize					R		Y_R		M		
Nsize									M		
Narea									M*		
AR	R*		Y_R*	O_R	R*		Y_R*			F_R	M_R
Aheight											
Awidth											
HWR	R*	Y	Y_R	O_R	R*		Y_R*	O_R		F_R*	M_R
BF	R		Y_R*								
BL			Y_R*								
Vdiam	U			O_U*		O					
SizeR	R*		Y_R		R*		Y_R				
VOR			Y_R								
CR											
EI											
NSI	R*	Y	Y_R*	O_R*	R*		Y_R	O_R*	M*	F_R*	M_R*
MLN	R*	Y	Y_R*	O_R*	R*		Y_R	O_R*		F_R*	M_R*
Sample Size	278	233	114	115	282	259	102	149	261	193	60

R and U indicate significantly positive and negative association of the variable with aneurysm rupture, respectively. Asterisks refer to significant difference after adjustment for multiple testing. O, Y, M, and F refer to a significant association of the variable with aneurysm rupture for older and younger, male and female patients, respectively. Empty cells indicate no statistically significant difference

($p < 0.001$), and MLN ($p < 0.001$). For aneurysms located at the ACOM, additionally a larger MWSSnorm ($p = 0.004$), larger BF ($p = 0.01$), and smaller WSSmin ($p = 0.004$) were associated with rupture. In case of the MCA-BIF, ruptured aneurysms had a larger mean OSI ($p < 0.001$), WSS in the parent vessel ($p = 0.009$) and were larger ($p = 0.03$; see Tab. 4 and 6 in the Online Suppl. Material).

For aneurysms at the ACOM, compared to older patients, younger patients had aneurysms that were subjected to a lower minimum WSS ($p = 0.05$), had a larger HWR ($p = 0.007$), NSI ($p = 0.004$), and MLN ($p = 0.03$). At the MCA-BIF, aneurysms of younger patients had a larger mean OSI ($p = 0.04$) and smaller neck diameter ($p = 0.03$) and parent vessel diameter ($p = 0.03$). When comparing ruptured and unruptured aneurysms in the subgroup of young and old patients, most of

the parameters that had been associated with rupture for the overall comparison irrespective of age group, were also associated with rupture for the subgroup-analyses (see Tab. 4–7 in the Online Suppl. Material).

With respect to gender differences, male aneurysms at the MCA-BIF were characterized by a larger inflow rate ($p = 0.001$), kinetic energy ($p = 0.005$), mean velocity ($p = 0.005$), vorticity ($p = 0.04$), maximum and mean WSS ($p = 0.01$ and 0.02), vortex coreline length ($p = 0.04$), and Vmax ($p = 0.002$). Besides, they were larger ($p = 0.04$), had a larger neck size and area ($p = 0.03$ and 0.006), and were less spherical ($p = 0.006$) compared to aneurysms of female patients. Figure 1 illustrates the observed associations: The left, ruptured male aneurysm is characterized by a complex, non-spherical shape and a high, complex flow field. In contrast, the unruptured
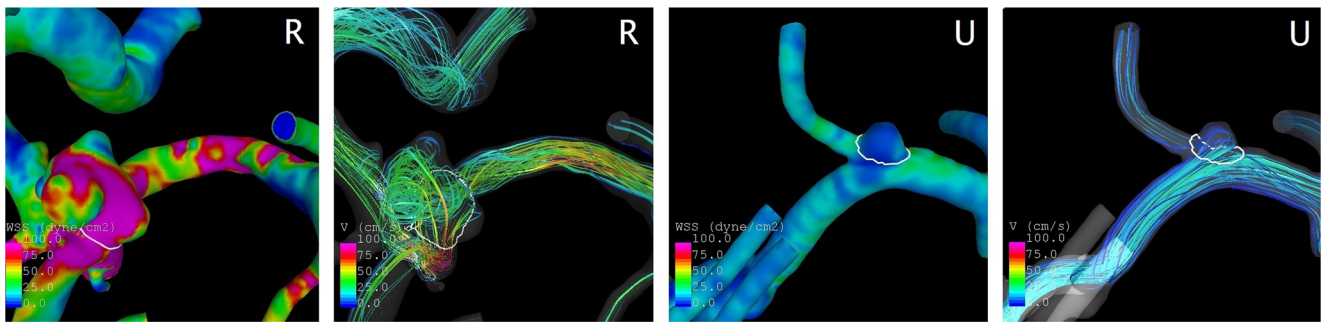
Fig. 1 Results of CFD simulations for two MCA bifurcation aneurysms. The left two images show the WSS distribution and streamlines for a non-spherical, ruptured male aneurysm with high flow conditions, the right two images for a spherical, unruptured female aneurysm with low flow conditions

female aneurysm shown at the right has a spherical shape and a low, non-complex flow field.

Similar to the analysis for the subgroups of age, when comparing parameters between ruptured and unruptured aneurysms in the subgroups of male and female patients, overall the same associations with rupture were found as for the comparison of all ruptured and unruptured aneurysms irrespective of gender (see Tab. 6, 8, and 9 in the Online Suppl. Material).

Bifurcation versus sidewall aneurysms

Rupture rates between sidewall and bifurcation aneurysms were significantly different at the MCA (rupture rates 0 vs. 0.27, $p = 0.02$) and the PCOM (0.37 vs. 0.54, $p = 0.006$, see Table 5). When looking at the hemodynamics, bifurcation aneurysms at the MCA had a larger inflow concentration index (ICI, $p = 0.02$), inflow (Q, $p = 0.03$), velocity ($p = 0.02$), MWSSnorm ($p = 0.01$), and Vmax ($p = 0.01$), but a lower LSA ($p = 0.04$). PCOM bifurcation aneurysms had a significantly larger SCI ($p = 0.02$), OSImax ($p = 0.003$), MWSSnorm ($p = 0.01$), and podent ($p = 0.03$, see Table 6). With respect to the morphology, bifurcation aneurysms both at the MCA and PCOM were larger ($p = 0.03$ for MCA, $p = 0.01$ for PCOM) and had a larger MLN ($p = 0.04$ and $p < 0.001$) compared to sidewall aneurysms. Bifurcation aneurysms at the MCA were further characterized by larger necks (Nsize, $p = 0.004$, Narea, $p = 0.03$). For the PCOM, bifurcation aneurysms had a larger height ($p = 0.01$), HWR ($p < 0.001$), BL ($p = 0.004$), and were less spherical (NSI, $p = 0.003$).

Discussion

The analysis of hemodynamic, morphological, and patient-related parameters in 1931 aneurysms showed associations of several of the considered variables with aneurysm rupture.

Hemodynamic conditions and aneurysm morphologies associated with rupture

Ruptured aneurysms were overall exposed to a hemodynamic environment of larger and more complex flows characterized by a larger mean velocity, mean and maximum WSS, mean and maximum OSI, podent, and corelen. Interestingly, when normalizing the mean WSS with respect to the WSS in the parent artery, it was significantly lower in ruptured aneurysms, which is in agreement with previous studies [6, 8]. Regarding morphology, ruptured aneurysms were overall larger and more irregular in shape indicated by a larger AR, NSI, and MLN, which is consistent with data from the literature [6, 8].

The interaction test indicated a possibly different influence of Vmax, BL, and MLN on the rupture risk depending on aneurysm location. For all other parameters, the association with aneurysm rupture risk was independent of the aneurysm location. When comparing aneurysm hemodynamics and morphology by location, the results were consistent with the overall comparison. Variables that had significantly larger values for ruptured aneurysms at one location were not significantly lower for aneurysms at another location. At the same

Table 5 Results of comparison of rupture rates for subgroups of bifurcation versus sidewall aneurysms by location

	Rupture rate sidewall	Rupture rate bifurcation	p value	Method	Signf.	Sample size (sidewall/bifurcation)
ACA-ACOM	0.19	0.39	0.24	ChiSq		75 (26/49)
ICA-ACHOR	0.11	0.15	1	Fis		49 (9/40)
ICA-OPH	0.09	0.04	0.10	ChiSq		301(171/130)
MCA	0	0.27	0.02	Fis	*	348 (16/332)
PCOM	0.37	0.54	0.006	ChiSq	*	293 (98/195)

ChiSq refers to a comparison of rupture rates by a Chi-squares test, Fis to a comparison using Fisher's exact test

Table 6 Summary of univariate comparison of morphological and hemodynamic parameters by for bifurcation versus sidewall PCOM and MCA aneurysms

	PCOM	MCA
ICI		BIF
Q		BIF
KE		
SR		
VE		BIF
VO		
VD		
WSSmax		
WSSmin		
WSSmean		
LSA		LAT
SCI	BIF	
OSImax	BIF*	
OSImean		
WSSves		
WSSnorm		
MWSSnorm	BIF	BIF
corelen		
podent	BIF	
Vmax		BIF
Avol		
Asize	BIF	BIF
Nsize		BIF
Narea		BIF
AR		
Aheight	BIF	
Awidth		
HWR	BIF*	
BF		
BL	BIF*	
Vdiam		
SizeR		
VOR		
CR		
EI		
NSI	BIF*	
MLN	BIF*	BIF

BIF and LAT refer to a significant association of the variable with aneurysm rupture for bifurcation and sidewall aneurysms, respectively. Asterisks refer to significant difference after adjustment for multiple testing. Empty cells indicate no statistically significant difference

time, the varying sample sizes for different locations could partly explain why some parameters were significantly different at some locations, but not at others. These results indicate that overall, the same mechanisms seem to be leading to aneurysm rupture independent of the aneurysm location.

Age

In our data, aneurysms harbored by patients younger than 55 years had a significantly higher rupture rate compared to aneurysms of older patients. In the literature, the influence of patient's age on aneurysm rupture risk is not clear. Whereas some studies report a higher risk for older patients [19, 20] others are in agreement with the findings reported here [21–23]. Based on the indication of an influence of the of aneurysm location on the association between age and rupture risk, five aneurysm locations were identified with significantly higher rupture rates for younger patients. The analysis of hemodynamics and morphology at two of these locations (ACOM and MCA-BIF) revealed that hemodynamic and morphological characteristics being overall associated with a higher rupture rate, were also associated with a higher rupture rate in the subgroups of aneurysms harbored by younger or older patients, respectively. Furthermore, for ACOM aneurysms, younger age was associated with a more complex aneurysm shape, which was in turn related to ruptured aneurysms. Similarly, the two hemodynamic parameters that were associated with younger age (WSSmin for ACOM aneurysms and OSImean for MCA-BIF aneurysms) were related to rupture. Hence, aneurysms of younger patients show similar trends as ruptured aneurysms, which could explain the higher rupture rate for younger patients.

Gender

While females have a higher prevalence of cerebral aneurysms [1], the association between the risk of their rupture and gender remains unclear with one meta-analysis describing a higher rupture risk for females [24] and a population based study stating no association between gender and rupture risk [23]. Moreover, similar ratios of females to males in two autopsy studies including patients with ruptured and unruptured aneurysms, respectively, indicate that a higher rate of SAH patients among females is related to a higher prevalence of aneurysms and not to a higher rupture rate [25, 26]. With respect to gender-related risk factors for formation and rupture of aneurysms, also results from studies investigating the influence of hormone replacement therapy or oral contraceptives remain conflicting [27–30]. In our data, we found a significantly higher rupture rate for male aneurysms. When stratifying by aneurysm location, significant differences in rupture rates between genders were found at the ICA-BIF, ICA-OPH, and MCA-BIF. The analysis of hemodynamics and morphology of aneurysms at the MCA-BIF revealed that male aneurysms were exposed to an environment of high flow conditions described by higher inflow, kinetic energy, mean velocity, vorticity, maximum WSS, mean WSS, vortex core line length, and peak velocity. Besides, they were larger and less spherical. Interestingly, they also had a larger neck, which was

in the overall cohort related to unruptured aneurysms. The adverse hemodynamic environment as well as the more complex shape were also characteristics of ruptured aneurysms. The higher rupture rate found in male MCA bifurcation aneurysms is therefore associated with high flow conditions in those aneurysms. The underlying morphology of larger, more complexly shaped aneurysms might be related to such hemodynamic environment.

Bifurcation versus sidewall aneurysms

For aneurysms at the MCA and PCOM, bifurcation aneurysms had a significantly larger rupture rate compared to sidewall aneurysms. The larger rupture rates were associated with a more adverse hemodynamic environment characterized by more concentrated and more complex flows for bifurcation aneurysms at those two locations. Furthermore, bifurcation aneurysms were more complex in shape.

Implications

Overall, we found higher rupture rates at certain locations for aneurysms harbored by males vs. females (ICA-BIF, ICA-OPH, MCA-BIF), aneurysms harbored by younger vs. older patients (ACOM, BA-DIST-PROX, ICA-BIF, ICA-SHYP, MCA-BIF), and bifurcation vs. sidewall aneurysms (MCA, PCOM). At the same time, in general ruptured aneurysms were associated with an adverse hemodynamic environment and more complex aneurysm shapes. Based on our findings, it seems that those conditions are more likely to occur for aneurysms harbored by younger, male patients and for bifurcation aneurysms, which leads to the higher rupture rates observed for these subgroups. Although the findings of a more adverse hemodynamic environment and more complex shapes for ruptured aneurysms were generally consistent throughout different aneurysm locations, these mechanisms seem to be particularly important at certain locations, resulting in significantly different rupture rates for the analyzed subgroups at those locations.

Limitations

This study is subject to several limitations. Regarding the CFD simulations, blood was modeled as a Newtonian fluid and vessel wall motion was neglected. Besides, it was assumed that aneurysms do not largely change in shape due to the event of rupture.

Regarding the differences associated with gender, the higher rupture rate in male aneurysms could potentially be related to a selection bias. Females have for instance a higher prevalence of migraine headache [31] and might undergo diagnostic cerebral imaging more often resulting in a higher number of discovered unruptured aneurysms compared to

males. The same aspect could potentially also apply to older patients who might receive diagnostic angiographic imaging more often than younger patients. Apart from a selection bias, the higher rupture rate in males might also be related to a higher occurrence of smoking and alcohol consumption in this population [32], which are associated with a higher rupture risk [2]. The effect of smoking on the rupture risk could also depend on gender [33]. In the presented study, information about alcohol consumption was not available. For a subset of 411 aneurysms with known information about the patient's classification as smoker or non-smoker, 12 aneurysms were harbored by smoking patients. All of them were females, indicating that at least for this subset, the significantly higher rupture rate of male aneurysms was not related to the smoking status.

Conclusion

The presented analysis of data from a large patient cohort shows that high flow conditions and a more complex aneurysm shape are associated with rupture. A higher rupture risk and similar hemodynamic and morphological characteristics were also found for younger and male patients as well as bifurcation aneurysms.

Compliance with ethical standards

Conflict of interest The authors declare that they have no conflict of interest.

Ethical approval All procedures performed in studies involving human participants were in accordance with the ethical standards of the institutional and/or national research committee and with the 1964 Helsinki declaration and its later amendments or comparable ethical standards.

Informed consent For this type of study formal consent is not required.

References

1. Vlak MH, Algra A, Brandenburg R, Rinkel GJ (2011) Prevalence of unruptured intracranial aneurysms, with emphasis on sex, age, comorbidity, country, and time period: a systematic review and meta-analysis. Lancet Neurol 10:626–636. https://doi.org/10.1016/s1474-4422(11)70109-0
2. Juvela S, Poussa K, Lehto H, Porras M (2013) Natural history of unruptured intracranial aneurysms: a long-term follow-up study. Stroke 44:2414–2421. https://doi.org/10.1161/strokeaha.113.001838
3. Rivero-Arias O, Gray A, Wolstenholme J (2010) Burden of disease and costs of aneurysmal subarachnoid haemorrhage (aSAH) in the

United Kingdom. Cost Eff Resour Alloc 8:6. https://doi.org/10.1186/1478-7547-8-6

4. Gabriel RA, Kim H, Sidney S, McCulloch CE, Singh V, Johnston SC, Ko NU, Achrol AS, Zaroff JG, Young WL (2010) Ten-year detection rate of brain arteriovenous malformations in a large, multiethnic, defined population. Stroke 41:21–26. https://doi.org/10.1161/STROKEAHA.109.566018

5. Longo M, Granata F, Racchiusa S, Mormina E, Grasso G, Longo GM, Garufi G, Salpietro FM, Alafaci C (2017) Role of hemodynamic forces in unruptured intracranial aneurysms: an overview of a complex scenario. World Neurosurg 105:632–642. https://doi.org/10.1016/j.wneu.2017.06.035

6. Xiang J, Natarajan SK, Tremmel M, Ma D, Mocco J, Hopkins LN, Siddiqui AH, Levy EI, Meng H (2011) Hemodynamic-morphologic discriminants for intracranial aneurysm rupture. Stroke 42:144–152

7. Miura Y, Ishida F, Umeda Y, Tanemura H, Suzuki H, Matsushima S, Shimosaka S, Taki W (2013) Low wall shear stress is independently associated with the rupture status of middle cerebral artery aneurysms. Stroke 44:519–521. https://doi.org/10.1161/STROKEAHA.112.675306

8. Jing L, Fan J, Wang Y, Li H, Wang S, Yang X, Zhang Y (2015) Morphologic and hemodynamic analysis in the patients with multiple intracranial aneurysms: ruptured versus unruptured. PLoS One 10:e0132494. https://doi.org/10.1371/journal.pone.0132494

9. Lv N, Wang C, Karmonik C, Fang Y, Xu J, Yu Y, Cao W, Liu J, Huang Q (2016) Morphological and hemodynamic discriminators for rupture status in posterior communicating artery aneurysms. PLoS One 11:e0149906. https://doi.org/10.1371/journal.pone.0149906

10. Ishibashi T, Murayama Y, Urashima M, Saguchi T, Ebara M, Arakawa H, Irie K, Takao H, Abe T (2009) Unruptured intracranial aneurysms: incidence of rupture and risk factors. Stroke 40:313–316. https://doi.org/10.1161/STROKEAHA.108.521674

11. Chung BJ, Mut F, Putman C, Hamzei-Sichani F, Brinjikji W, Kallmes D, Jimenez CM, Cebral JR (2018) Identification of hostile hemodynamics and geometries of cerebral aneurysms: a case-control study. AJNR Am J Neuroradiol. https://doi.org/10.3174/ajnr.A5764

12. Mut F, Löhner R, Chien A, Tateshima S, Viñuela F, Putman C, Cebral JR (2011) Computational hemodynamics framework for the analysis of cerebral aneurysms. Int J Numer Method Biomed Eng 27:822–839

13. Byrne G, Mut F, Cebral JR (2014) Quantifying the large-scale hemodynamics of intracranial aneurysms. AJNR Am J Neuroradiol 35:333–338 https://doi.org/10.3174/ajnr.A3678

14. Ma B, Harbaugh RE, Raghavan ML (2004) Three-dimensional geometrical characterization of cerebral aneurysms. Ann Biomed Eng 32:264–273

15. Raghavan ML, Ma B, Harbaugh RE (2005) Quantified aneurysm shape and rupture risk. J Neurosurg 102:355–362

16. Chung BJ, Doddasomayajula R, Mut F, Detmer F, Pritz MB, Hamzei-Sichani F, Brinjikji W, Kallmes DF, Jimenez CM, Putman CM, Cebral JR (2017) Angioarchitectures and hemodynamic characteristics of posterior communicating artery aneurysms and their association with rupture status. Am J Neuroradiol 38:2111–2118. https://doi.org/10.3174/ajnr.A5358

17. Benjamini Y, Hochberg Y (1995) Controlling the false discovery rate: a practical and powerful approach to multiple testing. J R Stat Soc Ser B Methodol 57:289–300

18. R Core Team (2016) R: a language and environment for statistical computing. Version 3.3.3, R Foundation for Statistical Computing, Vienna, Austria

19. Greving JP, Wermer MJ, Brown RD et al (2014) Development of the PHASES score for prediction of risk of rupture of intracranial aneurysms: a pooled analysis of six prospective cohort studies. Lancet Neurol 13:59–66. https://doi.org/10.1016/s1474-4422(13)70263-1

20. Backes D, Rinkel GJE, Greving JP, Velthuis BK, Murayama Y, Takao H, Ishibashi T, Igase M, terBrugge KG, Agid R, Jääskeläinen JE, Lindgren AE, Koivisto T, von und zu Fraunberg M, Matsubara S, Moroi J, Wong GKC, Abrigo JM, Igase K, Matsumoto K, Wermer MJH, van Walderveen MAA, Algra A, Vergouwen MDI (2017) ELAPSS score for prediction of risk of growth of unruptured intracranial aneurysms. Neurology 88:1600–1606. https://doi.org/10.1212/WNL.0000000000003865

21. Matsukawa H, Uemura A, Fujii M, Kamo M, Takahashi O, Sumiyoshi S (2013) Morphological and clinical risk factors for the rupture of anterior communicating artery aneurysms. J Neurosurg 118:978–983. https://doi.org/10.3171/2012.11.JNS121210

22. Wang G-X, Yu J-Y, Wen L, Zhang L, Mou KJ, Zhang D (2016) Risk factors for the rupture of middle cerebral artery bifurcation aneurysms using CT angiography. PLoS One 11:e0166654. https://doi.org/10.1371/journal.pone.0166654

23. Juvela S, Porras M, Poussa K (2000) Natural history of unruptured intracranial aneurysms: probability of and risk factors for aneurysm rupture. J Neurosurg 93:379–387. https://doi.org/10.3171/jns.2000.93.3.0379

24. Wermer MJH, van der Schaaf IC, Algra A, Rinkel GJE (2007) Risk of rupture of unruptured intracranial aneurysms in relation to patient and aneurysm characteristics: an updated meta-analysis. Stroke 38:1404–1410. https://doi.org/10.1161/01.STR.0000260955.51401.cd

25. Inagawa T, Hirano A (1990) Autopsy study of unruptured incidental intracranial aneurysms. Surg Neurol 34:361–365

26. Kongable GL, Lanzino G, Germanson TP, Truskowski LL, Alves WM, Torner JC, Kassell NF, the Participants (1996) Gender-related differences in aneurysmal subarachnoid hemorrhage. J Neurosurg 84:43–48. https://doi.org/10.3171/jns.1996.84.1.0043

27. Mhurchu CN, Anderson C, Jamrozik K, Hankey G, Dunbabin D, Australasian Cooperative Research on Subarachnoid Hemorrhage Study (ACROSS) Group (2001) Hormonal factors and risk of aneurysmal subarachnoid hemorrhage: an international population-based, case-control study. Stroke 32:606–612

28. Jamous MA, Nagahiro S, Kitazato KT, Satomi J, Satoh K (2005) Role of estrogen deficiency in the formation and progression of cerebral aneurysms. Part I: experimental study of the effect of oophorectomy in rats. J Neurosurg 103:1046–1051. https://doi.org/10.3171/jns.2005.103.6.1046

29. Jamous MA, Nagahiro S, Kitazato KT, Tamura T, Kuwayama K, Satoh K (2005) Role of estrogen deficiency in the formation and progression of cerebral aneurysms. Part II: experimental study of the effects of hormone replacement therapy in rats. J Neurosurg 103:1052–1057. https://doi.org/10.3171/jns.2005.103.6.1052

30. Qureshi AI, Malik AA, Saeed O, Defillo A, Sherr GT, Suri MFK (2016) Hormone replacement therapy and the risk of subarachnoid hemorrhage in postmenopausal women. J Neurosurg 124:45–50. https://doi.org/10.3171/2014.12.JNS142329

31. Lipton RB, Stewart WF, Diamond S, Diamond ML, Reed M (2001) Prevalence and burden of migraine in the United States: data from the American Migraine Study II. Headache 41:646–657

32. Juvela S, Lehto H (2015) Risk factors for all-cause death after diagnosis of unruptured intracranial aneurysms. Neurology 84:456–463. https://doi.org/10.1212/WNL.0000000000001207

33. Lindekleiv H, Sandvei MS, Njølstad I et al (2011) Sex differences in risk factors for aneurysmal subarachnoid hemorrhage: a cohort study. Neurology 76:637–643. https://doi.org/10.1212/WNL.0b013e31820c30d3